

Controlling the Electrochemical Activity of Dahlia-like β - NiS@rGO by the Interface Polarization

Yiqing Wei^{1, 3†}, Xuefeng Zou^{2†}, Chao Cen², Bin Zhang⁴, Bin Xiang^{*1}, Jiangyu Hao¹,
Bo Wang⁵, Mingsen Deng^{*2}, Qin Hu¹, Shicheng Wei^{*5}

¹Chemistry and Chemical Engineering, Chongqing University, Chongqing 400044, P. R. China.

²Guizhou Provincial Key Laboratory of Computational Nano-Material Science, Guizhou Education University, Guiyang 550018, P. R. China.

³ Center of Quantum Materials & Devices and College of Physics, Chongqing University, Chongqing 401331, P. R. China

⁴Analytical and Testing Center of Chongqing University, Chongqing 400044, P. R. China.

⁵National Key Laboratory for Remanufacturing, Army Academy of Armored Forces, Beijing 100072, P. R. China.

*Corresponding author.

TEL: 18502332795. E-mail: xiangbin@cqu.edu.cn (Bin Xiang),

TEL: 13995609825. E-mail: deng@gznc.edu.cn (Mingsen Deng),

TEL: 13364017376. E-mail: wsc33333@163.com (Shicheng Wei).

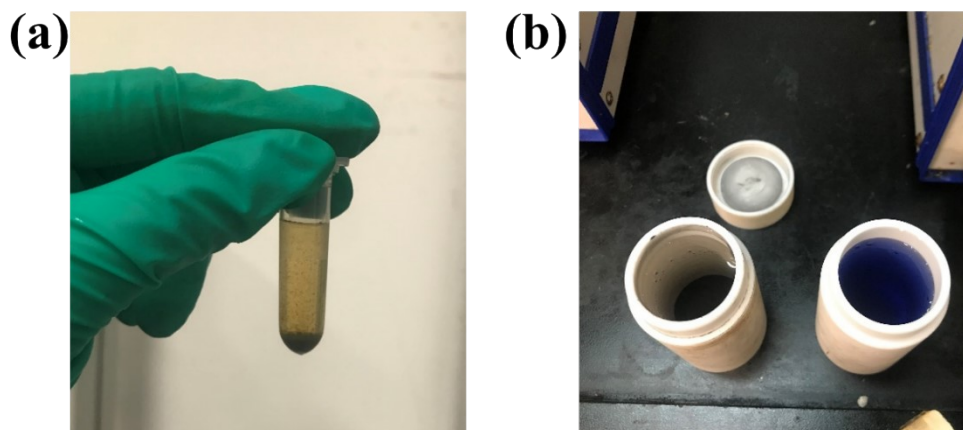


Fig. S1. (a) The image of CuS precipitates. (b) The image of reaction system (the left is with ammonia, and the right is without ammonia).

The generation of S^{2-} ions can be demonstrated by the formation of black-brown precipitates of CuS (Fig. S1a and the left of Fig. S1b), where the 3,3'-thiodipropionic acid was solely dissolved in the ammonia solution and put into a Teflon-lined stainless autoclave to react for 20 h at 200 °C. After the solution was cooled to room temperature, the $CuSO_4 \cdot 5H_2O$ reagent was added to the cooled solution, and dark-brown precipitates of CuS were produced. On the contrary, in the absence of ammonia, the system is blue ($CuSO_4 \cdot 5H_2O$) and there is no black-brown precipitates (CuS) to collect (see in the right of Fig. S1b), which indicates that no S^{2-} is produced. This means that ammonia is essential to produce S^{2-} .

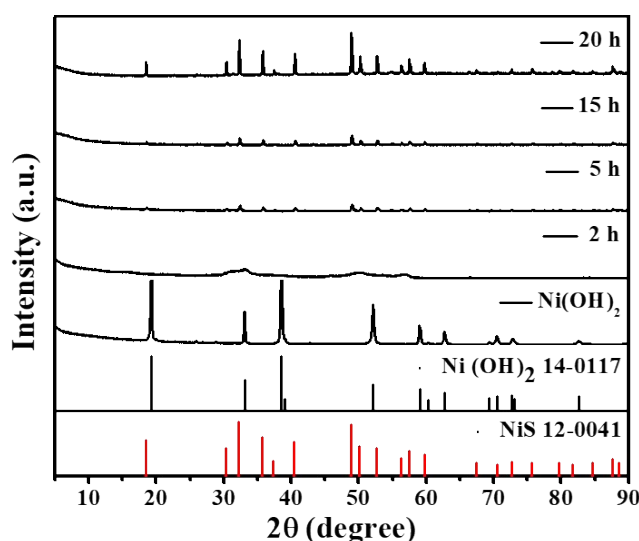


Fig. S2. The XRD patterns of the products collected at different time intervals (2, 5, 15, and 20 h) and $Ni(OH)_2$.

From the Fig. S2, after 1 hour of reaction time, no product was discovered. When increased to 2 h, the XRD pattern of the obtained products has a broad peak, and the peak position is consistent

with β -NiS (PDF#12-0041) in the standard card, figuring that NiS has been initially formed. And the peaks in the XRD pattern gradually narrowed and sharpened with the further increase in reaction time, exposing an increasing crystallinity. When the reaction time was 20 h, β -NiS having a good crystallinity was gathered.

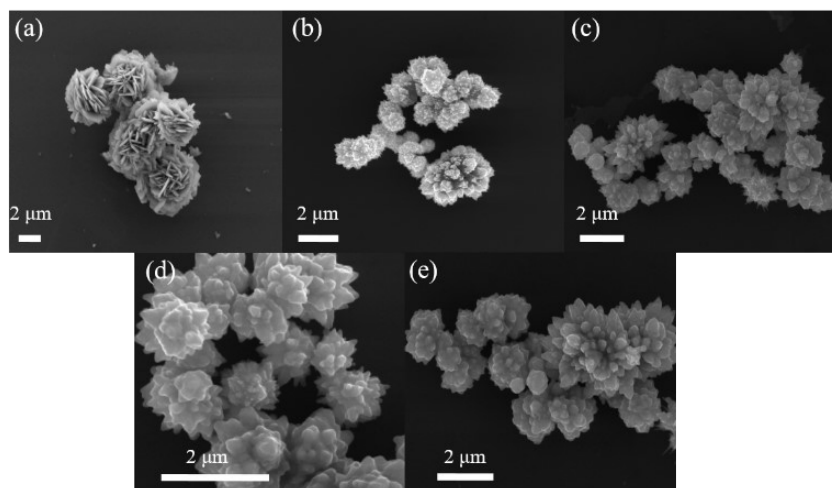


Fig. S3. (a) SEM images of Ni(OH)₂, (b-e) SEM images of the products synthesized at different reaction times (2, 5, 15, and 20 h).

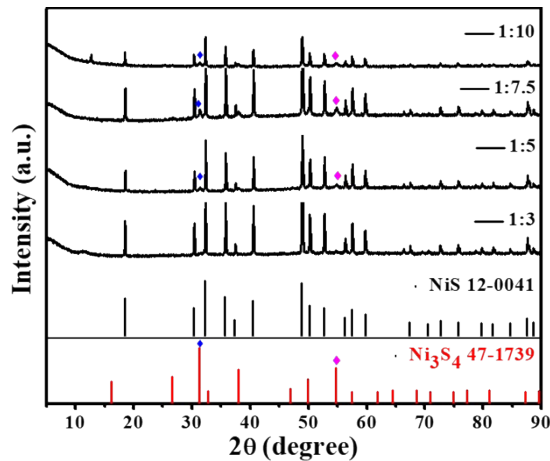


Fig. S4. XRD patterns of the as-prepared products with different molar ratio of Ni and S sources. The blue and purple points represent the (311) and (440) lattice planes of Ni₃S₄ (PDF #47-1739), respectively.

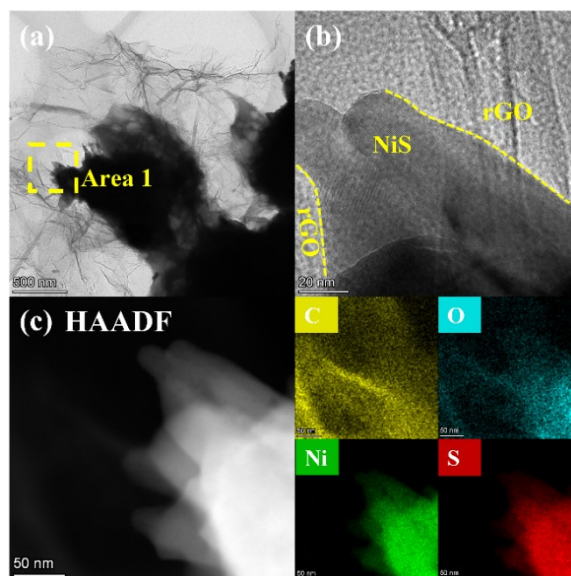


Fig. S5. (a) TEM image, (b) HRTEM image, and (c) EDS mapping of β -NiS@rGO. The yellow dotted line indicates the interface between β -NiS and rGO.

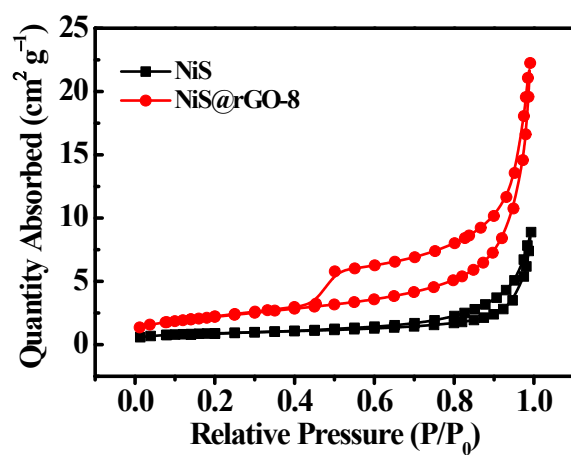


Fig. S6. N₂ absorption-desorption isotherm curves of NiS and NiS@rGO-8.

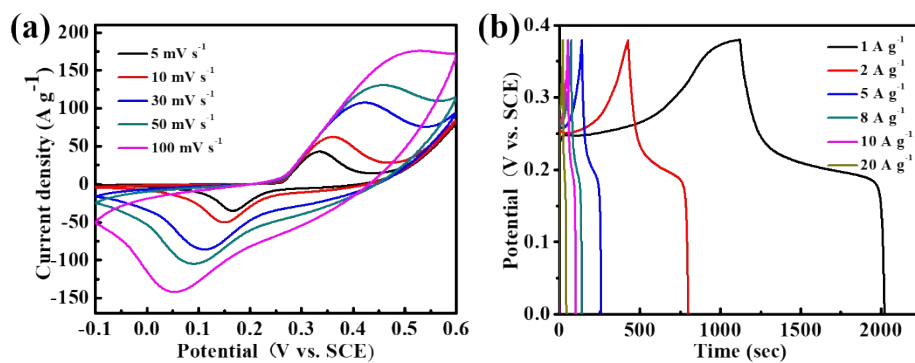


Fig. S7. (a) CV curves of β -NiS electrode at various scan rates from 5 to 100 mV s^{-1} , (b) GCD curves of β -NiS electrode at different current densities from 1 to 20 A g^{-1} .

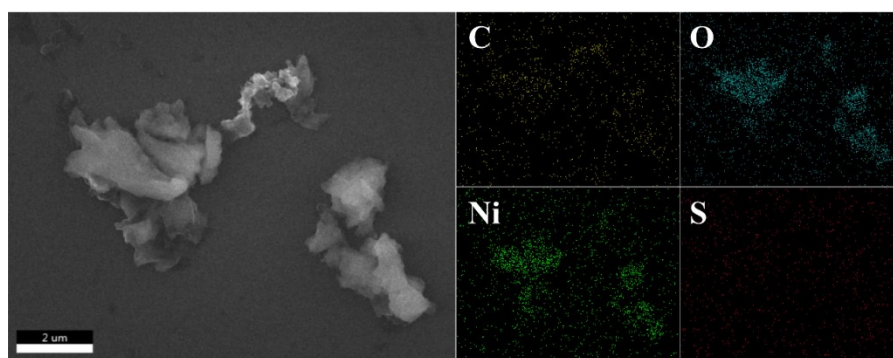


Fig. S8. SEM image and corresponding EDS mapping of β -NiS@rGO sample after 3000 cycles at 10 A g^{-1} .

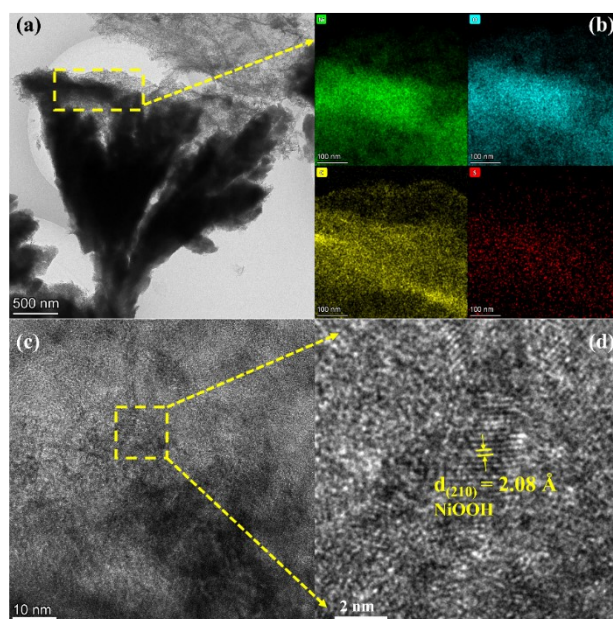


Fig. S9. (a) TEM image, (b) EDS mapping, (c, d) HRTEM image for β -NiS@rGO sample after 3000 cycles at 10 A g^{-1} .

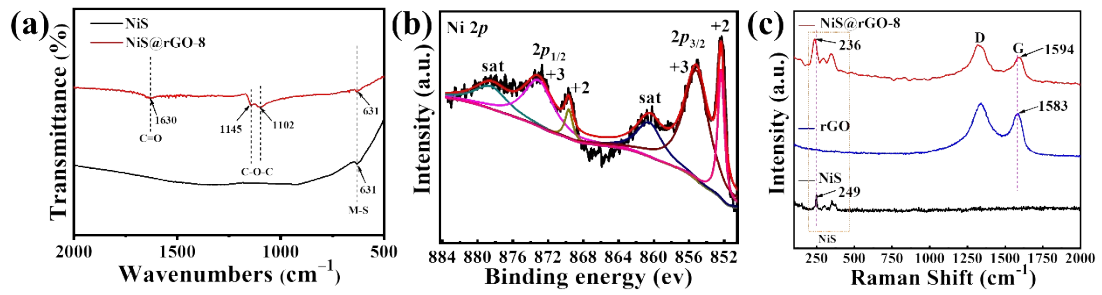


Fig. S10. (a) FT-IR spectrum of β -NiS and β -NiS@rGO-8, (b) Ni2p XPS spectrum of β -NiS, (c) Raman spectra of NiS, rGO and β -NiS@rGO-8.

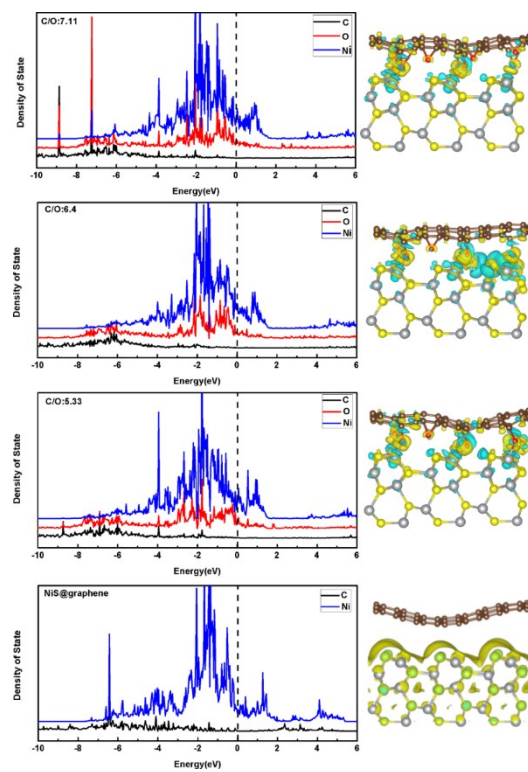


Fig. S11. The density of state (DOS) and differential charge density distribution of β -NiS(110) @ rGO with different C and O ratios.

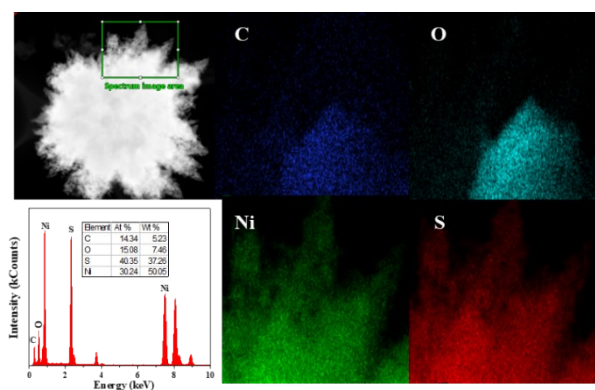


Fig. S12. EDS spectrum and mapping of NiS@rGO-2.

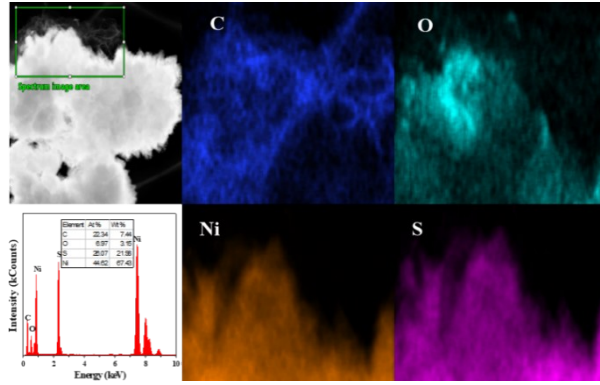


Fig. S13. EDS spectrum and mapping of NiS@rGO-5.

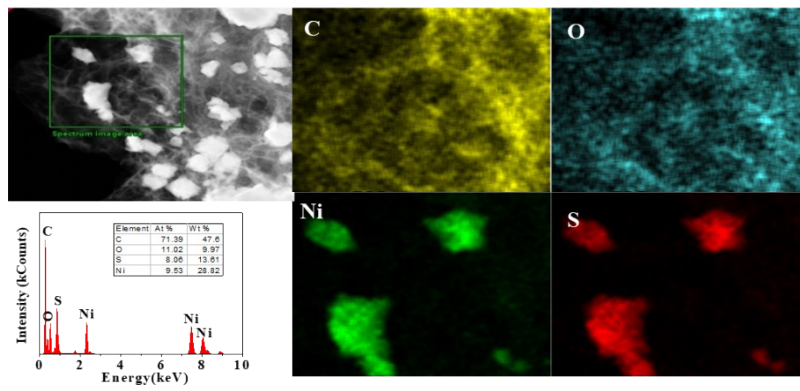


Fig. S14. EDS spectrum and mapping of NiS@rGO-8.

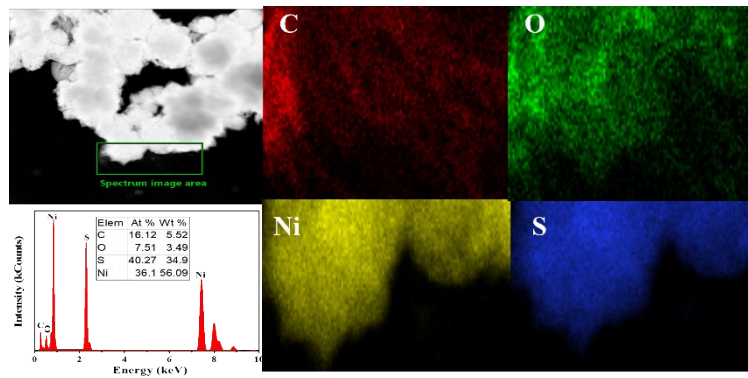


Fig. S15. EDS spectrum and mapping of NiS@rGO-10.

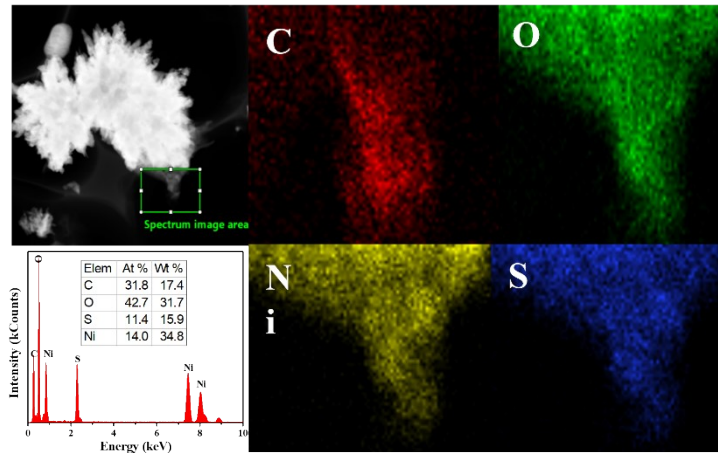


Fig. S16. EDS spectrum and mapping of NiS@rGO-20.

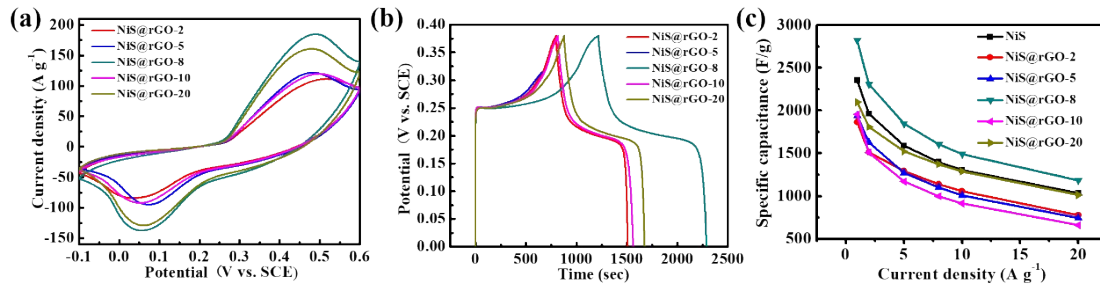


Fig. S17. (a) and (b) CV curves at 5 mV s^{-1} and GCD curves at 1 A g^{-1} of composites formed by β -NiS with different contents of rGO (marked as β -NiS@rGO-2, β -NiS@rGO-5, β -NiS@rGO-8, β -NiS@rGO-10, and β -NiS@rGO-20). (c) Specific capacitance of different materials at various current densities.

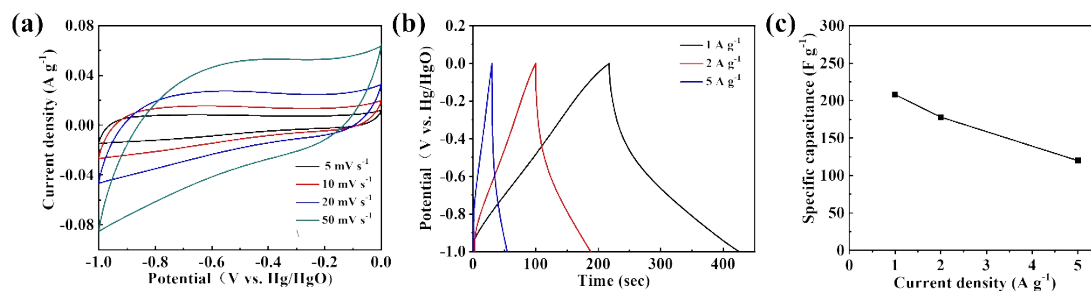


Fig. S18. (a) CV curves of rGO at various scan rates from 5 to 50 mV s^{-1} , (b) GCD curves of rGO at different current densities from 1 to 5 A g^{-1} , (c) Specific capacitance of rGO at various current densities.

The CV curves at various scanning rates in Fig. S16a are approximate rectangle with wide Faraday redox peaks, which suggests that rGO has the energy storage behavior of electric double

layers and pseudocapacitors. They are attributed to ion adsorption-desorption and reversible redox reactions of oxygen-containing groups (such as -OH, C=O, and -COOH), respectively. This is also reflected in GCD curves with atypical triangles (Fig. S16b). The specific capacitance of rGO is calculated from the GCDs and plotted in Fig. S16c, and it is found that the specific capacitance decreases as the current density increases.

Table S1. The loads of active substance in different system.

Three-electrode system		Two-electrode system	
active substance.	load (mg)	active substance.	load (mg)
NiS	1.6		
NiS@rGO-2	1.6	NiS@rGO-8	$m_+ = 2.1$
NiS@rGO-5	1.7		
NiS@rGO-8	1.6		
NiS@rGO-10	2.1	rGO	$m_- = 10.8$
NiS@rGO-20	1.8		

Table S2. The calculated specific capacities.

Current density (A g ⁻¹)	Specific capacity			
	β -NiS		β -NiS@rGO-8	
	(mAh g ⁻¹)	(F g ⁻¹)	(mAh g ⁻¹)	(F g ⁻¹)
1	248.59	2355.04	297.77	2820.95
2	207.22	1963.11	243.69	2308.68
5	167.87	1590.39	195.22	1849.47
8	147.76	1399.79	169.31	1604.00
10	137.76	1305.08	157.42	1491.32
20	109.09	1033.45	124.83	1182.61

Table S3. The content of C, O, Ni and S in β -NiS@rGO-2, β -NiS@rGO-5, β -NiS@rGO-8, β -NiS@rGO-10 and β -NiS@rGO-20 detected by EDS.

Materials	Content (at%)				
	C	O	Ni	S	C/O
β -NiS@rGO-2	14.34	15.08	30.24	40.35	0.95
β -NiS@rGO-5	22.34	6.97	44.62	26.07	3.21
β -NiS@rGO-8	71.39	11.02	9.53	8.06	6.48
β -NiS@rGO-10	16.12	7.51	36.10	40.27	2.15
β -NiS@rGO-20	31.83	42.71	14.01	11.45	0.75